ORGANOMETALLICS

pubs.acs.org/Organometallics Article

Six-Membered Iridacycles with Five Nitrogen Atoms in the Ring

J. Drake Johnson, Andrew J. King, Fu-Sheng Wang, and Aleksandr V. Zhukhovitskiy*

Cite This: *Organometallics* 2024, 43, 1593−1599

Read Online

ACCESS | Metrics & More | Article Recommendations | Supporting Information

ABSTRACT: Catalytic diazene metathesis is a fundamental inorganic transformation that remains unrealized despite its potential value, given the photochemical properties of the diazene functional group. Diazenes and polymers comprising them have a multitude of functions ranging from molecular motors to dyes and actuators, and catalytic diazene metathesis would be an enabling tool for their synthesis. However, current approaches to diazene metathesis founded on the [2+2] cycloaddition/elimination mechanism have not been able to achieve catalyst turnover. Alternative mechanisms for this metathesis based on insertion/elimination could circumvent this challenge. As a crucial step toward realizing this mechanism, we have synthesized several complexes that resemble potential intermediates in a proposed insertion/elimination mechanism for diazene metathesis: specifically, these complexes feature six-membered metallocycles comprising one iridium and five contiguous nitrogen atoms. These complexes can be prepared in a straightforward manner through the reaction of *N*-alkyl triazoline diones with an iridium imido complex within minutes at room temperature. Furthermore, redox reactivity of these complexes is explored leading to the formation of novel azo imides. This work provides an alternative starting point for mechanism and catalyst design toward catalytic diazene metathesis.

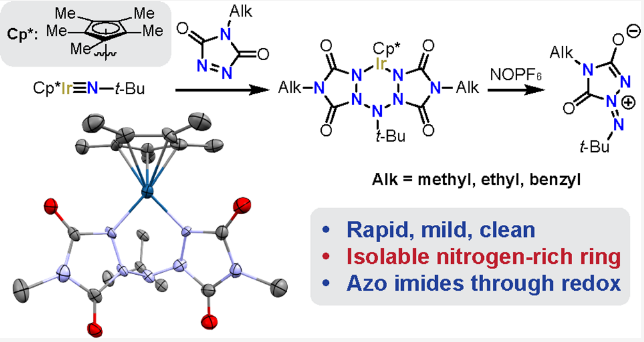

Catalytic diazene metathesis (CDM) is a potentially powerful fundamental inorganic transformation that has not been realized to date. CDM could facilitate the synthesis of innumerable high-value products: azo-dyes,[1,2] photoswitches and actuating polymers,[3] molecular motors,[4] and radical initiators.[5] Because diazenes represent a stimulus-responsive handle desirable for many applications, CDM promises far-reaching benefits across many disciplines. Currently, diazene homometathesis has only been observed under extreme pressures (20−40 GPa) within an engineered crystalline lattice, as reported by Zheng, Kang, and co-workers.[6] Catalysis may enable this metathesis to occur under more accessible conditions. En route to this goal, several examples of stoichiometric metathesis of diazenes with carbenes have been reported. The laboratories of Hegedus[7,8] and McElwee-White[9−11] demonstrated this reactivity with chromium and tungsten alkylidenes. More recently, experimental and computational investigations into the reactivity of the second-generation Grubbs catalyst toward diazenes were also published by the groups of Nicholas and of Jawiczuk and Trzaskowski.[12,13] Each of the aforementioned systems are thought to operate via a [2+2] cycloaddition/elimination mechanism analogous to that proposed by Chauvin for olefin metathesis,[14] but none have achieved catalyst turnover. We therefore hypothesized that the energy barrier for a Chauvin-type CDM mechanism is too high to be viable.

Cleavage of nitrogen−nitrogen double bonds, central to diazene metathesis, has also been explored in other contexts. Bimetallic tantalum and niobium complexes have been shown to stoichiometrically cleave diazenes to form di-imido complexes, as reported by Cotton and co-workers;[15,16] Mashima, Tsurugi, and co-workers have described similar reactivity with ditungsten complexes.[17] Fürstner and co-workers have explored metathesis-like reactivity of diazonium salts with transition metal alkylidynes and diazenes with metallocarbenes generated from diazocarbonyl compounds.[18,19] Meanwhile Tonks and co-workers demonstrated catalytic diazene cleavage with titanium, vanadium, and tungsten complexes toward the synthesis of imines, pyrroles, and pyrazoles.[20−35] Yet, although these precedents teach us valuable lessons about diazene reactivity, they cannot be readily adapted to homometathesis of diazenes. These observations compelled us to explore alternative mechanisms toward CDM. Building on our recent insights in the realm of carbodiimide ring-opening metathesis polymerization (CDI ROMP),[36,37] we set out to explore the possibility of an

Received: April 21, 2024
Revised: June 17, 2024
Accepted: June 17, 2024
Published: July 1, 2024

https://doi.org/10.1021/acs.organomet.4c00163

alternative—insertion/elimination—mechanism to accomplish the analogous diazene ROMP (Figure 1A)[36] with extensions to other forms of CDM. For such a mechanism to be possible, unprecedented six-membered rings composed of a transition metal and five nitrogen atoms must be accessible. Hence, we set out to address the viability of such intermediates.

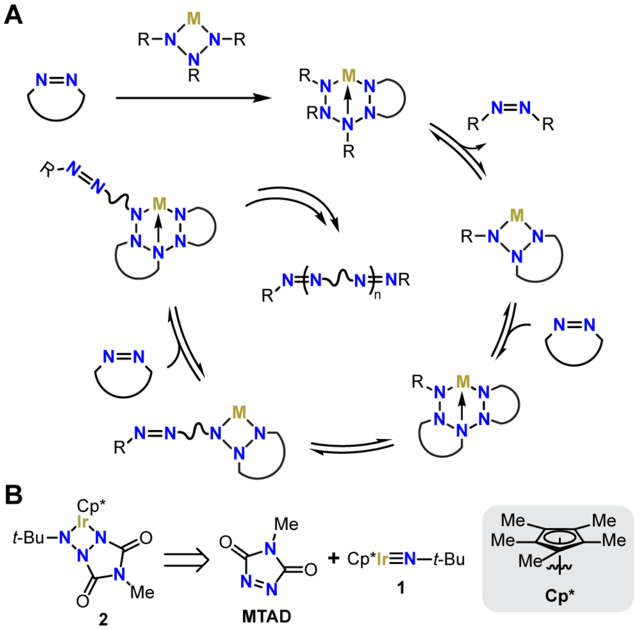

Figure 1. A. A proposed route for catalytic diazene ROMP. "M" refers to a transition metal fragment, with additional ligands omitted for clarity. B. The synthesis of an initiator for diazene ROMP that is structurally analogous to the initiator used for CDI ROMP.

■ RESULTS AND DISCUSSION

Specifically, we hypothesized that treatment of iridium(III) imido species **1**[38] with triazoline diones (TADs)[39,40] would furnish four-membered metallocycles (e.g., **2**, Figure 1B), which would be good starting points to explore the target diazene insertion/elimination reactivity. Our investigation began with 4-methyl-1,2,4-triazoline-3,5-dione (**MTAD**, Figure 2A). When stoichiometric **MTAD** was added to a solution of **1** at 23 °C in benzene, complete conversion of **MTAD** and 50% conversion of **1** occurred within 5 min, as observed by ^{1}H nuclear magnetic resonance (^{1}H NMR) spectroscopy. These changes corresponded to the appearance of three new resonances in the ^{1}H NMR spectrum, indicative of a single symmetric product. Addition of another equivalent of **MTAD** under the same conditions led to the complete consumption of **1** and **MTAD** and virtually quantitative formation of the same product, which suggested a 2:1 **MTAD**/**1** stoichiometry in this product (Figure 2B). X-ray crystallography of the crystals grown from the concentrated reaction mixture (at 23 °C, 24 h) revealed the product to be **3** (Figures 2C, S1, and S2); remarkably, **3** features a six-membered iridacycle with five nitrogen atoms, which maps onto the target intermediate of CDM. The X-ray crystal structure of **3** was consistent with ^{1}H, ^{13}C, and two-dimensional (2D) NMR analysis (Figures S3–

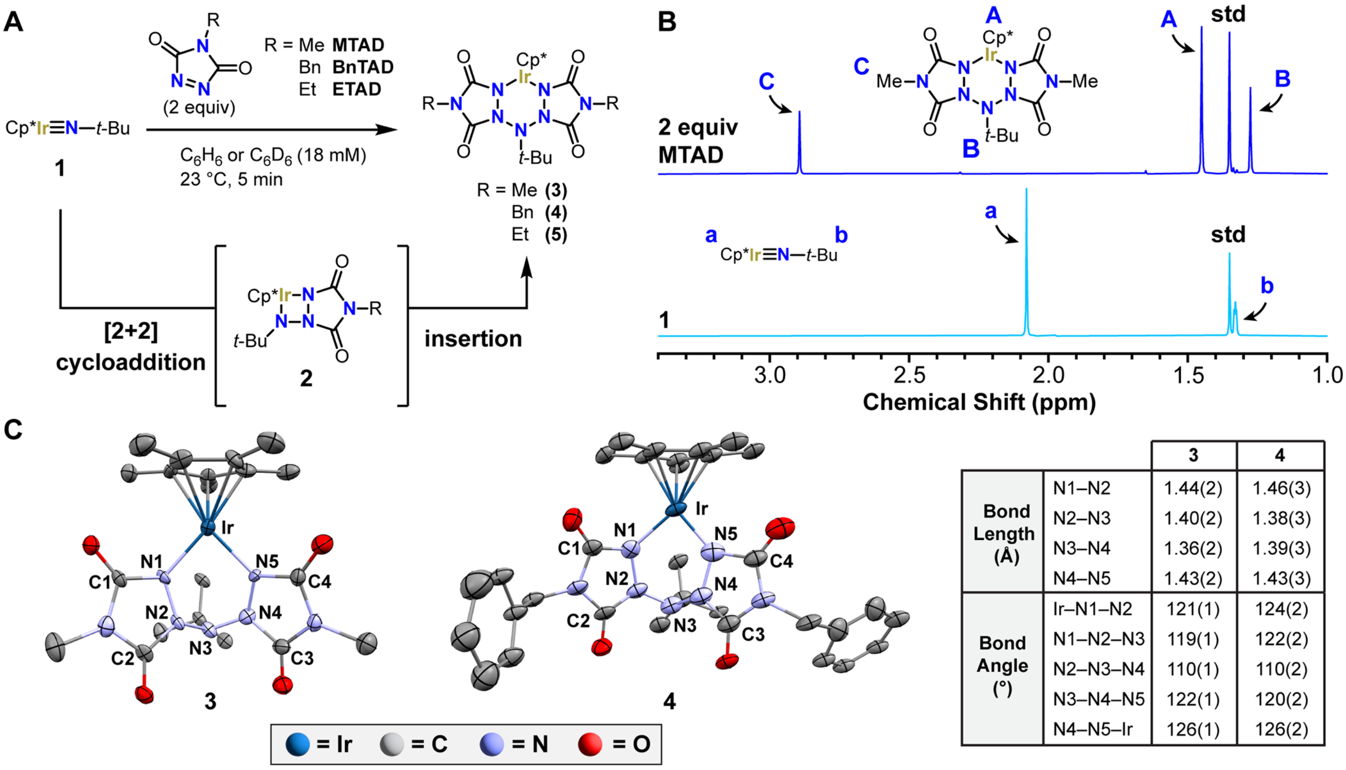

		3	4
Bond Length (Å)	N1–N2	1.44(2)	1.46(3)
	N2–N3	1.40(2)	1.38(3)
	N3–N4	1.36(2)	1.39(3)
	N4–N5	1.43(2)	1.43(3)
Bond Angle (°)	Ir–N1–N2	121(1)	124(2)
	N1–N2–N3	119(1)	122(2)
	N2–N3–N4	110(1)	110(2)
	N3–N4–N5	122(1)	120(2)
	N4–N5–Ir	126(1)	126(2)

Figure 2. A. Proposed reaction and possible intermediate **2** in the synthesis of **3**–**5** from the corresponding TAD and **1**. B. ^{1}H NMR spectra (C_6D_6, 23 °C, 500 MHz) showing the conversion of **1** to **3**. std = 1,3,5-tri-*tert*-butylbenzene. C. X-ray crystal structures of **3** and **4** (50% ORTEP, R = 0.097 for **3**, R = 0.118 for **4**), with hydrogen atoms and solvent molecules omitted for clarity. Bond lengths and angles of interest are displayed in table format. Data for **4** are reported as the average bond lengths and angles of the three molecules present in the asymmetric unit (Figure S11).

https://doi.org/10.1021/acs.organomet.4c00163

S7), as well as high-resolution mass spectrometry (HRMS, Figure S8).

We hypothesized that **3** formed via a two-step process (Figure 2A): a [2+2] cycloaddition between **1** and one equivalent of **MTAD** to yield **2**, followed by insertion of a second equivalent of **MTAD** into the Ir–N(*t*-Bu) bond of **2**. Similar reactivity had been reported by Bergman and co-workers for **1** with dimethyl acetylene dicarboxylate instead of **MTAD**, although in that case, reductive elimination followed the insertion step to form an iridium pyrrole complex.[38]

Upon further investigation, we found this reactivity to be generalizable to other alkyl TADs such as 4-benzyl and 4-ethyl-1,2,4-triazoline-3,5-dione (**BnTAD** and **ETAD**), forming **4** and **5**, respectively. Single crystals of **4**—formed at 23 °C from vapor diffusion of hexanes into a concentrated solution of **4** in benzene—proved structurally analogous to **3** (Figures 2C, S9–S17). Recrystallization of **5** proved challenging due to decomposition; however, HRMS and $^1H/^{13}C$/2D NMR spectroscopy data (Figures S18–S23) for this compound are analogous to those of **3** and **4**, supporting its structural assignment.

The crystal structures of **3** and **4** (Figure 2C, S1, S2, S9–S11) revealed several notable characteristics. In both complexes, the Ir–N1–N2, N1–N2–N3, N3–N4–N5, and N4–N5–Ir bond angles were between 120° and 126°, while the N2–N3–N4 bond angles were ∼110°. The former are consistent with sp^2 hybridization of the nitrogen atoms N1, N2, N4, and N5, while the latter is more consistent with sp^3 hybridization of N3. There is also inherent curvature in both complexes, with the *tert*-butyl substituent projected out from the convex face (Figures S2, S10). This asymmetry explains the chemical inequivalence of the benzyl and methylene protons of **4** and **5** observed in ^1H NMR spectra (Figures S12, S18).

Another feature of these complexes is that the N–N bonds associated with the triazoline dione fragments in **3** and **4** are somewhat elongated compared to those in the hydrogenated form of **MTAD** (**MTAD-H$_2$**): the latter has an N–N bond length of 1.419 Å,[41] while the corresponding N–N bond lengths are 1.44(2) Å and 1.43(2) Å in **3** and 1.46(3) Å and 1.43(3) Å in **4** (Figure 2C). Such bond lengthening suggests overlap of the corresponding N1–N2 and N4–N5 σ^* orbitals with the nonbonding orbital localized on the *tert*-butylamido nitrogen (N3). This hypothesis is supported by the approximated dihedral angles of the N3 lone pair electrons and the N1–N2 and N4–N5 bonds of **3** (176.1° and 152.5°) and **4** (160.8° and 178.0°) (see discussion in SI), as well as the fact that N2–N3 and N3–N4 bonds of **3** (1.40(2) Å and 1.36(2) Å) and **4** (1.38(3) Å and 1.39(3) Å) are shorter than N1–N2 and N4–N5 bonds. This pattern of bond lengths is particularly notable as a structural foreshadowing that ring-opening may be feasible in such systems, though we do not observe it here. The frontier orbitals of **3** were investigated with density functional theory (DFT, see "Computational methodology" in SI), which found the highest occupied molecular orbital (HOMO, Figure S24) encompassed the IrN_5 portion of the complex, while the lowest unoccupied molecular orbital (LUMO, Figure S24) was centered mainly on the IrCp* system. The corresponding HOMO–LUMO gap was found to be ∼1.5 eV.

It is important to note that the insertion step of our proposed mechanism for this reaction occurs only into the Ir–N(*t*-Bu) bond of **2** (a, Figure 3), rather than the Ir–N(C=O) bond (b). Presumably, the reason for this regioselectivity of insertion is due to the kinetic—and potentially thermodynamic—preference of the electrophilic diazene moiety in **MTAD** for insertion at the more nucleophilic N(*t*-Bu) rather than N(C=O) site. To explore this hypothesis, the ground states of **3** and **3′** were investigated with DFT. These computations revealed **3** to be ∼17 kcal/mol lower in energy than **3′**, supporting our reasoning. Unfortunately, ring-opening metathesis cannot occur from the resulting complex **3** as it would from **3′** (Figure 3).

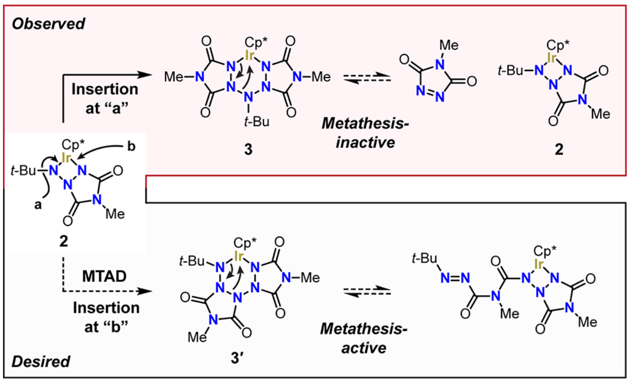

Figure 3. Possible regiochemistries of MTAD insertion into the Ir–N bonds of **2** and the theoretical further reactivity of the resulting complexes.

Though complexes **3**–**5** do not effect metathesis, they hold significance as a series of isolable 6-membered rings containing five nitrogen atoms, which map onto possible intermediates of CDM. Furthermore, such structures, with or without metals, are exceedingly rare in the literature.[42] As such, these complexes provide new opportunities to study the bonding characteristics and chemical reactivity of compounds that feature nitrogen atom chains and rings, which are, with some exceptions,[43–48] thermally unstable outside of extreme conditions.[49–52] Complexes **3** and **4** persist in the solid state when stored at −35 °C in a glovebox and could be handled and analyzed without apparent degradation under an inert atmosphere at 23 °C for at least 3 h. In solution at 23 °C, degradation of **3** and **4** begins after ∼36 h. Interestingly, **5** showed ∼10% degradation in the solid state after 2 days at −35 °C (Figure S25).

Given the well-known explosion hazard of some nitrogen-rich species, we sought to determine if our complexes shared such characteristics.[46,53] We began our investigation of this question in the context of **3** with thermogravimetric analysis (TGA, Figure S26) and differential scanning calorimetry (DSC, Figure S27). TGA revealed that at 160 °C, **3** rapidly lost ∼15% mass, which was followed by a gradual loss of an additional 45% mass over the next 440 °C. At 600 °C, mass loss had reached a plateau, leaving ∼40% of its mass in the form of char, likely containing iridium. In accord with the first mass loss in TGA, DSC (Figure S27) exhibited an exotherm with an onset of 120 °C and an associated decomposition enthalpy of 299 J/g. Notably, this value is below the 500 J/g threshold over which a substance must be screened for explosivity, according to United Nations shipping standards,[54] and well below that of other azodicarbonyl species.[55] No other major exotherms were observed within the 25–400 °C temperature range tested. We also conducted a qualitative hammer test using 10 mg of the complex. No explosion was noted in this experiment (Supplementary Videos 1 and 2).

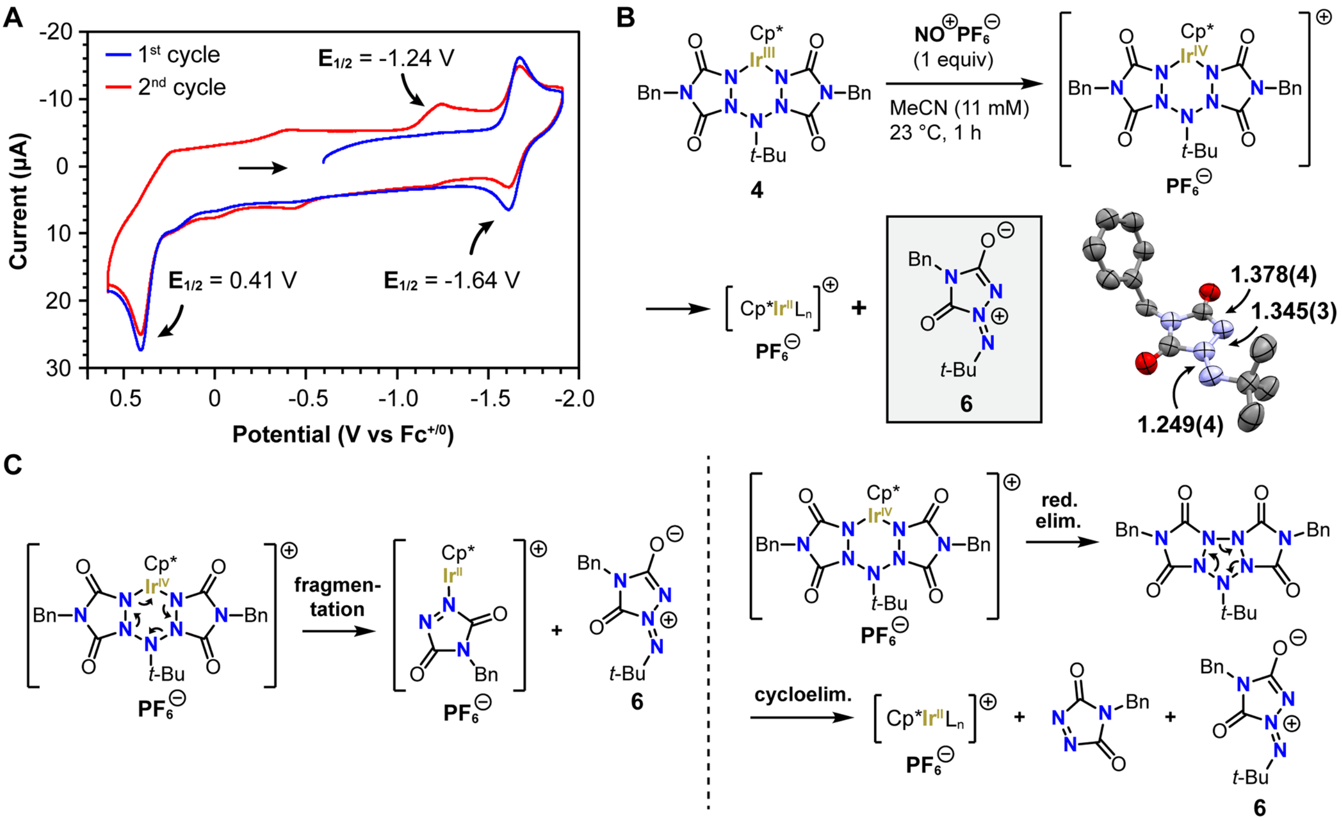

Figure 4. A. CV of **3**: [**3**] = 0.5 mM in MeCN, 0.25 M NBu_4PF_6, 200 mV/s, Ag wire pseudoelectrode, 3 mm glassy carbon electrodes. B. Chemical oxidation of **4**, which produces azo imide **6**. Adjacent is its X-ray structure (50% ORTEPs, R = 0.0614), with hydrogen atoms and disorder omitted for clarity. Relevant bond lengths are indicated with arrows. C. Two possible mechanisms postulated for the formation of **6** induced by oxidization of **4**.

Overall, the experiments above indicate that **3** does not pose an explosion hazard despite the high nitrogen content in the iridacycle portion of this molecule.

Given the unusual IrN_5 iridacycle present in **3**−**5**, we wondered if redox chemistry of these complexes could produce novel nitrogen-rich heterocycles. Specifically, we hypothesized that the oxidation of the Ir(III) metal center to Ir(IV) would induce an N−N bond forming reductive elimination. To evaluate the relevant redox potentials, **3** was subjected to cyclic voltammetry (CV) in acetonitrile (Figure 4A). An irreversible oxidation event was observed at a potential of 0.41 V (relative to $Fc^{+/0}$), which also led to a new reduction event at −1.24 V. We attempted to accomplish a similar oxidative event using a convenient chemical oxidant—nitrosonium hexafluorophosphate ($NOPF_6$)—with a sufficiently high redox potential of 0.87 V in acetonitrile (Figure 4B).[56] By ^1H NMR spectroscopy, full conversion of **3** was observed over 1 h when treated with stoichiometric $NOPF_6$ at 23 °C. This reaction yielded two major products, which were separable based on their relative solubility but proved challenging to identify based on mass spectrometry and NMR spectroscopy; crystallization of these products was similarly unsuccessful. We hypothesized that the analogous products derived from **4** would be more amenable to crystallization. Thus, **4** was oxidized in the same manner, which produced a similar distribution of products based on NMR analysis (Figure S28) and, indeed, enabled the recrystallization of **6** (Figures 4B, S29, and S30) from a −35 °C solution in methyl *tert*-butyl ether (MTBE). The crystal structure shown in Figure 4B shows atom connectivity in agreement with $^1H/^{13}C$/2D NMR (Figures S31−S33), and the N−N and N−C bond lengths are suggestive of electron delocalization between these atoms, as expected of **6**. From these results, we believe **6** is an azo imide/azimine. Azo imides are a class of compounds that serve as 1,3-dipole building blocks for the synthesis of heterocycles containing three contiguous nitrogen atoms,[57−60] as precursors to triaziridines,[61,62] and as dyes.[63] We hypothesize that this product arises through a reductive elimination occurring from the oxidized form of **4**, potentially through one of the mechanisms shown in Figure 4C. This reactivity opens a new pathway to these compounds, which could widen the scope of accessible azo imides.

■ CONCLUSIONS

In this report, we have demonstrated novel reactivity of TAD derivatives with iridium imido species that produces metallocycles with five nitrogen atoms in the ring. This reaction proceeds rapidly and cleanly at room temperature and is generalizable to alkyl TADs. The similarities between these complexes and the intermediates proposed for the insertion/elimination mechanism for diazene metathesis provide a starting point for catalyst design to enable productive metathesis. Furthermore, the redox behavior of these complexes provides a new pathway to azo imide 1,3-dipoles. Lastly, because **3**−**5** contain unique six-membered rings with five nitrogen atoms, these complexes offer valuable insights into bonding in nitrogen-rich molecules.

https://doi.org/10.1021/acs.organomet.4c00163

■ ASSOCIATED CONTENT

Supporting Information

The Supporting Information is available free of charge at https://pubs.acs.org/doi/10.1021/acs.organomet.4c00163.

Materials and methods, experimental procedures, computational details, Supplementary Figures S1–S33 referenced in the main text, crystallographic data, spectral characterization, and thermal characterization (PDF)

Supplementary Video 1: Control hammer test on stage (MP4)

Supplementary Video 2: Hammer test on 10 mg of **3** (MP4)

Accession Codes

CCDC 2349924 and 2349927–2349928 contain the supplementary crystallographic data for this paper. These data can be obtained free of charge via www.ccdc.cam.ac.uk/data_request/cif, or by emailing data_request@ccdc.cam.ac.uk, or by contacting The Cambridge Crystallographic Data Centre, 12 Union Road, Cambridge CB2 1EZ, UK; fax: +44 1223 336033.

■ AUTHOR INFORMATION

Corresponding Author

Aleksandr V. Zhukhovitskiy − *Department of Chemistry, University of North Carolina at Chapel Hill, Chapel Hill, North Carolina 27599, United States;* orcid.org/0000-0002-3873-4179; Email: alexzhuk@email.unc.edu

Authors

J. Drake Johnson − *Department of Chemistry, University of North Carolina at Chapel Hill, Chapel Hill, North Carolina 27599, United States*

Andrew J. King − *Department of Chemistry, University of North Carolina at Chapel Hill, Chapel Hill, North Carolina 27599, United States*

Fu-Sheng Wang − *Department of Chemistry, University of North Carolina at Chapel Hill, Chapel Hill, North Carolina 27599, United States;* orcid.org/0000-0002-4659-986X

Complete contact information is available at: https://pubs.acs.org/10.1021/acs.organomet.4c00163

Author Contributions

A.V.Z. directed the project, and A.V.Z. and J.D.J. designed the experiments. J.D.J. conducted all experiments. A.J.K. solved the crystal structures and provided valuable discussion. F.-S.W. performed all computational experiments. J.D.J. and A.V.Z. wrote the manuscript. All authors analyzed the data.

Notes

The authors declare no competing financial interest.

■ ACKNOWLEDGMENTS

The material presented in this manuscript is based on work supported by the American Chemical Society Petroleum Research Fund under Grant # 65640-DNI7 and the National Science Foundation under Grant # CHE-2203499. The authors thank Prof. Wei You's group (UNC-CH, Chemistry) for use of their TGA instrument. The authors thank Charlotte Montgomery in Prof. Jillian Dempsey's group (UNC-CH, Chemistry) for carrying out cyclic voltammetry measurements. The authors thank the Soft Matter Characterization Core lab (UNC-CH, Chemistry) for the use of their DSC. The authors thank Dr. Marc ter Horst, Dr. Nuwanthika Kumarage, and Dr. Luke Fulton for NMR discussion, and Dr. Brandie Ehrmann for MS advice (UNC-CH, Chemistry). The authors thank Dr. Chun-Hsing (Josh) Chen (UNC-CH, Chemistry) for his assistance in collecting and analyzing X-ray crystallography data. The authors thank the UNC Chemistry NMR facility (NSF Grant No. CHE-0922858), the UNC Chemistry Mass Spectrometry facility (NIH Grant No. R35GM118055), and the UNC X-ray Core Laboratory (NSF Grant No. CHE-2117287) for the use of their instrumentation. This work was performed in part at the Chapel Hill Analytical and Nanofabrication Laboratory (CHANL), a member of the North Carolina Research Triangle Nanotechnology Network (RTNN), which is supported by the NSF Grant No. ECCS-2025064, as part of the National Nanotechnology Coordinated Infrastructure (NNCI). The authors thank the UNC Research Computing group for providing computation resources and support.

■ REFERENCES

(1) Allen, R. L. M. The Chemistry of Azo Dyes. In *Colour Chemistry*; Springer US: Boston, MA, 1971; pp 21–36. DOI: 10.1007/978-1-4615-6663-2_3.

(2) Alsantali, R. I.; Raja, Q. A.; Alzahrani, A. Y. A.; Sadiq, A.; Naeem, N.; Mughal, E. U.; Al-Rooqi, M. M.; El Guesmi, N.; Moussa, Z.; Ahmed, S. A. Miscellaneous Azo Dyes: A Comprehensive Review on Recent Advancements in Biological and Industrial Applications. *Dyes Pigments* **2022**, *199*, No. 110050.

(3) Pang, X.; Lv, J. an; Zhu, C.; Qin, L.; Yu, Y. Photodeformable Azobenzene-Containing Liquid Crystal Polymers and Soft Actuators. *Adv. Mater.* **2019**, *31* (52), 1904224.

(4) Baroncini, M.; Silvi, S.; Credi, A. Photo- and Redox-Driven Artificial Molecular Motors. *Chem. Rev.* **2020**, *120* (1), 200–268.

(5) Moad, G. A Critical Assessment of the Kinetics and Mechanism of Initiation of Radical Polymerization with Commercially Available Dialkyldiazene Initiators. *Prog. Polym. Sci.* **2019**, *88*, 130–188.

(6) Gao, D.; Tang, X.; Zhang, C.; Wang, Y.; Yang, X.; Zhang, P.; Wang, X.; Xu, J.; Su, J.; Liu, F.; Dong, X.; Lin, X.; Yuan, B.; Hiraoka, N.; Zheng, H.; Kang, L.; Li, K.; Mao, H. Arylazo under Extreme Conditions: [2 + 2] Cycloaddition and Azo Metathesis. *J. Phys. Chem. C* **2023**, *127* (18), 8482–8492.

(7) Hegedus, L. S.; Kramer, A. Photolytic Reaction of Chromium Carbene Complexes with Azobenzenes. *Azo Metathesis. Organometallics* **1984**, *3* (8), 1263–1267.

(8) Hegedus, L. S.; Lundmark, B. R. The Course of the Reaction of Azobenzene with Chromium Carbene Complexes. *J. Am. Chem. Soc.* **1989**, *111* (26), 9194–9198.

(9) Sleiman, H. F.; McElwee-White, L.. Photochemical Azo Metathesis by Tungsten Carbene $(CO)_5W{=}C(OCH_3)CH_3$. Isolation of a of a Zwitterionic Intermediate. *J. Am. Chem. Soc.* **1988**, *110* (26), 8700–8701.

(10) Maxey, C. T.; McElwee-White, L. Formation of Diaziridines by Reaction of $(CO)_5W = C(OMe)Ph$ with Electron-Deficient Azo Compounds. *Organometallics* **1991**, *10* (6), 1913–1916.

(11) Maxey, C. T.; Sleiman, H. F.; Massey, S. T.; McElwee-White, L. Metathesis and Diaziridination Reactions of $(CO)_5W = C(OMe)$-*p*-XC_6H_4 with Cis-Azobenzene. Electronic and Solvent Effects. *J. Am. Chem. Soc.* **1992**, *114* (13), 5153–5160.

(12) Bousquet, L.; Nicholas, K. M. In Search of Alkene-Diazene Cross Metathesis. *J. Organomet. Chem.* **2019**, *899*, No. 120909.

(13) Jawiczuk, M.; Kuźmierkiewicz, N.; Nowacka, A. M.; Moreń, M.; Trzaskowski, B. Mechanistic, Computational Study of Alkene-Diazene Heterofunctional Cross-Metathesis Catalyzed by Ruthenium Complexes. *Organometallics* **2023**, *42* (2), 146–156.

(14) Jean-Louis Hérisson, P.; Chauvin, Y. Catalyse de transformation des oléfines par les complexes du tungstène. II.

Télomérisation des oléfines cycliques en présence d'oléfines acycliques. *Makromol. Chem.* **1971**, *141* (1), 161−176.

(15) Cotton, F. A.; Duraj, S. A.; Roth, W. J. A New Double Bond Metathesis Reaction: Conversion of an Niobium:Niobium and a Nitrogen:Nitrogen Bond into Two Niobium:Nitrogen Bonds. *J. Am. Chem. Soc.* **1984**, *106* (17), 4749−4751.

(16) Canich, J. A. M.; Albert Cotton, F.; Duraj, S. A.; Roth, W. J. The Preparation of $Ta_2Cl_6(PhN)_2(Me_2S)_2$ by Reaction of $Ta_2Cl_6(Me_2S)_3$ with PhNNPh: Crystal Structure of the Product. *Polyhedron* **1986**, *5* (3), 895−898.

(17) Ikeda, H.; Nishi, K.; Tsurugi, H.; Mashima, K. Metathesis Cleavage of an N = N Bond in Benzo[*c*]Cinnolines and Azobenzenes by Triply-Bonded Ditungsten Complexes. *Chem. Commun.* **2018**, *54* (30), 3709−3711.

(18) Lackner, A. D.; Fürstner, A. The Triple-Bond Metathesis of Aryldiazonium Salts: A Prospect for Dinitrogen Cleavage. *Angew. Chem., Int. Ed.* **2015**, *54* (43), 12814−12818.

(19) Tindall, D. J.; Werlé, C.; Goddard, R.; Philipps, P.; Farès, C.; Fürstner, A. Structure and Reactivity of Half-Sandwich Rh(+3) and Ir(+3) Carbene Complexes. Catalytic Metathesis of Azobenzene Derivatives. *J. Am. Chem. Soc.* **2018**, *140* (5), 1884−1893.

(20) Gilbert, Z. W.; Hue, R. J.; Tonks, I. A. Catalytic Formal [2 + 2+1] Synthesis of Pyrroles from Alkynes and Diazenes via Ti^{II}/Ti^{IV} Redox Catalysis. *Nat. Chem.* **2016**, *8* (1), 63−68.

(21) Davis-Gilbert, Z. W.; Tonks, I. A. A. Titanium Redox Catalysis: Insights and Applications of an Earth-Abundant Base Metal. *Dalton Trans.* **2017**, *46* (35), 11522−11528.

(22) Chiu, H.; Tonks, I. A. Trimethylsilyl-Protected Alkynes as Selective Cross-Coupling Partners in Titanium-Catalyzed [2 + 2+1] Pyrrole Synthesis. *Angew. Chem., Int. Ed.* **2018**, *57* (21), 6090−6094.

(23) Davis-Gilbert, Z. W.; Wen, X.; Goodpaster, J. D.; Tonks, I. A. Mechanism of Ti-Catalyzed Oxidative Nitrene Transfer in [2 + 2 + 1] Pyrrole Synthesis from Alkynes and Azobenzene. *J. Am. Chem. Soc.* **2018**, *140* (23), 7267−7281.

(24) Davis-Gilbert, Z. W.; Kawakita, K.; Blechschmidt, D. R.; Tsurugi, H.; Mashima, K.; Tonks, I. A. In Situ Catalyst Generation and Benchtop-Compatible Entry Points for Ti^{II}/Ti^{IV} Redox Catalytic Reactions. *Organometallics* **2018**, *37* (23), 4439−4445.

(25) Kawakita, K.; Beaumier, E. P.; Kakiuchi, Y.; Tsurugi, H.; Tonks, I. A.; Mashima, K. Bis(Imido)Vanadium(V)-Catalyzed [2 + 2+1] Coupling of Alkynes and Azobenzenes Giving Multisubstituted Pyrroles. *J. Am. Chem. Soc.* **2019**, *141* (10), 4194−4198.

(26) Chiu, H.-C.; See, X. Y.; Tonks, I. A. Dative Directing Group Effects in Ti-Catalyzed [2 + 2+1] Pyrrole Synthesis: Chemo- and Regioselective Alkyne Heterocoupling. *ACS Catal.* **2019**, *9* (1), 216−223.

(27) Beaumier, E. P.; Ott, A. A.; Wen, X.; Davis-Gilbert, Z. W.; Wheeler, T. A.; Topczewski, J. J.; Goodpaster, J. D.; Tonks, I. A. Ti-Catalyzed Ring-Opening Oxidative Amination of Methylenecyclopropanes with Diazenes. *Chem. Sci.* **2020**, *11* (27), 7204−7209.

(28) Cheng, Y.; Klein, C. K.; Tonks, I. A. Synthesis of Pentasubstituted 2-Aryl Pyrroles from Boryl and Stannyl Alkynes *via* One-Pot Sequential Ti-Catalyzed [2 + 2 + 1] Pyrrole Synthesis/Cross Coupling Reactions. *Chem. Sci.* **2020**, *11* (37), 10236−10242.

(29) Pearce, A. J.; Harkins, R. P.; Reiner, B. R.; Wotal, A. C.; Dunscomb, R. J.; Tonks, I. A. Multicomponent Pyrazole Synthesis from Alkynes, Nitriles, and Titanium Imido Complexes via Oxidatively Induced N−N Bond Coupling. *J. Am. Chem. Soc.* **2020**, *142* (9), 4390−4399.

(30) Pearce, A. J.; Cheng, Y.; Dunscomb, R. J.; Tonks, I. A. Generation of Masked Ti ^{II} Intermediates from Ti ^{IV} Amides via β-H Abstraction or Alkyne Deprotonation: An Example of Ti-Catalyzed Nitrene-Coupled Transfer Hydrogenation. *Organometallics* **2020**, *39* (21), 3771−3774.

(31) See, X. Y.; Wen, X.; Wheeler, T. A.; Klein, C. K.; Goodpaster, J. D.; Reiner, B. R.; Tonks, I. A. Iterative Supervised Principal Component Analysis Driven Ligand Design for Regioselective Ti-Catalyzed Pyrrole Synthesis. *ACS Catal.* **2020**, *10* (22), 13504−13517.

(32) Tonks, I. A. Ti-Catalyzed and -Mediated Oxidative Amination Reactions. *Acc. Chem. Res.* **2021**, *54* (17), 3476−3490.

(33) Huh, D. N.; Cheng, Y.; Frye, C. W.; Egger, D. T.; Tonks, I. A. Multicomponent Syntheses of 5- and 6-Membered Aromatic Heterocycles Using Group 4−8 Transition Metal Catalysts. *Chem. Sci.* **2021**, *12* (28), 9574−9590.

(34) Kaper, T.; Frye, C. W.; Tonks, I. A. Ti-Catalyzed Multicomponent Synthesis of Pyrroles Using Allene Coupling Partners. *Organometallics* **2023**, *42* (13), 1459−1464.

(35) Tsurugi, H.; Akiyama, T.; Frye, C. W.; Kakiuchi, Y.; Mashima, K.; Tonks, I. A. Evaluation of Tungsten Catalysis among Early Transition Metals for *N*-Aryl-2,3,4,5-tetraarylpyrrole Synthesis: Modular Access to N-Doped π-Conjugated Material Precursors. *Inorg. Chem.* **2024**, *63* (6), 3037−3046.

(36) Johnson, J. D.; Kaplan, S.; Toth, J.; Wang, Z.; Maw, M.; Sheiko, S.; Zhukhovitskiy, A. Carbodiimide Ring-Opening Metathesis Polymerization. *ACS Cent. Sci.* **2023**, *9*, 1104−1110.

(37) Johnson, J. D.; Zhukhovitskiy, A. V. Hetero-Ene Metathesis. *ACS Catal.* **2024**, *14* (1), 21−33.

(38) Glueck, D. S.; Wu, J.; Hollander, F. J.; Bergman, R. G. Monomeric (Pentamethylcyclopentadienyl)Iridium Imido Compounds: Synthesis, Structure, and Reactivity. *J. Am. Chem. Soc.* **1991**, *113* (6), 2041−2054.

(39) De Bruycker, K.; Billiet, S.; Houck, H. A.; Chattopadhyay, S.; Winne, J. M.; Du Prez, F. E. Triazolinediones as Highly Enabling Synthetic Tools. *Chem. Rev.* **2016**, *116* (6), 3919−3974.

(40) Okumura, M.; Sarlah, D. 4-Methyl-1,2,4-triazoline-3,5-dione. In *Encyclopedia of Reagents for Organic Synthesis*; Wiley, 2021; pp 1−11. DOI: 10.1002/047084289X.rn02375.

(41) Tenon, J. A.; Carles, M.; Aycard, J. P. 4-Méthyl-1,2,4-Triazolidine-3,5-Dione (Méthylurazole). *Acta Crystallogr. C* **1995**, *51* (7), 1440−1442.

(42) Hurst, D. T. Other Tetrazines and Pentazines. In *Comprehensive Heterocyclic Chemistry II*; Katritzky, A. R.; Rees, C. W.; Scriven, E. F. V., Eds.; Elsevier, 1996; pp 957−965. DOI: 10.1016/B978-008096518-5.00138-6.

(43) Vij, A.; Pavlovich, J. G.; Wilson, W. W.; Vij, V.; Christe, K. O. Experimental Detection of the Pentaazacyclopentadienide (Pentazolate) Anion, Cyclo-N_5^-. *Angew. Chem., Int. Ed.* **2002**, *41* (16), 3051.

(44) Benin, V.; Kaszynski, P.; Radziszewski, G. Arylpentazoles Revisited: Experimental and Theoretical Studies of 4-Hydroxyphenylpentazole and 4-Oxophenylpentazole Anion. *J. Org. Chem.* **2002**, *67* (4), 1354−1358.

(45) Carlqvist, P.; Östmark, H.; Brinck, T. The Stability of Arylpentazoles. *J. Phys. Chem. A* **2004**, *108* (36), 7463−7467.

(46) Klapötke, T. M.; Martin, F. A.; Stierstorfer, J. C_2N_{14}: An Energetic and Highly Sensitive Binary Azidotetrazole. *Angew. Chem., Int. Ed.* **2011**, *50* (18), 4227−4229.

(47) Zhang, C.; Sun, C.; Hu, B.; Yu, C.; Lu, M. Synthesis and Characterization of the Pentazolate Anion *Cyclo* -N_5^- in $(N_5)_6(H_3O)_3(NH_4)_4Cl$. *Science* **2017**, *355* (6323), 374−376.

(48) Bo, X.; Dong, Z.; Ding, Y. Arylpentazoles with Surprisingly High Kinetic Stability. *Chem. Commun.* **2021**, *57* (43), 5310−5313.

(49) Pirkle, W. H.; Stickler, J. C. Nitrogen-Backboned Polymers. *I. J. Am. Chem. Soc.* **1970**, *92* (25), 7497−7499.

(50) Wang, H.; Eremets, M. I.; Troyan, I.; Liu, H.; Ma, Y.; Vereecken, L. Nitrogen Backbone Oligomers. *Sci. Rep.* **2015**, *5* (1), 13239.

(51) Ishikawa, K. Perspectives on Functional Nitrogen Science and Plasma-Based in Situ Functionalization. *Jpn. J. Appl. Phys.* **2022**, *61*, No. SA0802.

(52) Laniel, D.; Trybel, F.; Yin, Y.; Fedotenko, T.; Khandarkhaeva, S.; Aslandukov, A.; Aprilis, G.; Abrikosov, A. I.; Bin Masood, T.; Giacobbe, C.; Bright, E. L.; Glazyrin, K.; Hanfland, M.; Wright, J.; Hotz, I.; Abrikosov, I. A.; Dubrovinsky, L.; Dubrovinskaia, N. Aromatic Hexazine $[N_6]_4^-$ Anion Featured in the Complex Structure of the High-Pressure Potassium Nitrogen Compound K_9N_{56}. *Nat. Chem.* **2023**, *15* (5), 641−646.

(53) Boyer, J. H. Handle Azide Compounds with Caution. *Chem. Eng. News* **1964**, *42*, 6.

(54) *Manual of Tests and Criteria*, seventh revised ed.; United Nations: New York, 2019.

(55) Berger, A.; Wehrstedt, K. D. Azodicarboxylates: Explosive Properties and DSC Measurements. *J. Loss Prev. Process Ind.* **2010**, *23* (6), 734−739.

(56) Connelly, N. G.; Geiger, W. E. Chemical Redox Agents for Organometallic Chemistry. *Chem. Rev.* **1996**, *96* (2), 877−910.

(57) Huisgen, R. 1,3-Dipolar Cycloadditions. Past and Future. *Angew. Chem., Int. Ed. Engl.* **1963**, *2* (10), 565−598.

(58) Challand, S. R.; Gait, S. F.; Rance, M. J.; Rees, C. W.; Storr, R. C. Azimines as 1,3-Dipoles. *J. Chem. Soc., Perkin Trans.* **1975**, *1* (1), 26−31.

(59) Egger, N.; Prewo, R.; Bieri, J. H.; Hoesch, L.; Dreiding, A. S. 1,2,3-Triazolidine Durch Cycloaddition von Aziminen an Olefine. *Helv. Chim. Acta* **1983**, *66* (5), 1608−1617.

(60) Koch, K.; Fahr, E. Amino-azimine Durch Addition von Aminonitrenen an α-Carbonyl-azo-Verbindungen. *Angew. Chem.* **1970**, *82* (15), 636−637.

(61) Kaupp, G.; Dengler, O.; Burger, K.; Rottegger, S. Stable Triaziridines. *Angew. Chem., Int. Ed. Engl.* **1985**, *24* (4), 341−342.

(62) Hoesch, L.; Leuenberger, C.; Hilpert, H.; Dreiding, A. S. Triaziridine. II. Erste Beispiele: 2, 3-Dialkyl-triaziridin-1-carbonsäurealkylester. *Helv. Chim. Acta* **1982**, *65* (8), 2682−2696.

(63) Boulton, A. J.; Henderson, N.; Powell, A. K.; Bracke, B. R. F.; Lenstra, A. T. H.; Vanmaele, L. J. Azimines Revisited: The Structure of a Magenta Dye. *J. Org. Chem.* **1991**, *56* (18), 5278−5281.

https://doi.org/10.1021/acs.organomet.4c00163